Published in final edited form as:
Biochem J. ; 420(3): 439–449. doi:10.1042/BJ20090214.

Role of nuclear encoded subunit Vb in the assembly and stability of Cytochrome C oxidase complex: Implications in Mitochondrial dysfunction and ROS Production

Domenico Galati[1,*], **Satish Srinivasan**[1,*], **Haider Raza**[1], **Subbuswamy K. Prabu**[1], **Michael Hardy**[2], **Chandran Karunakaran**[2], **Marcos Lopez**[2], **Balaraman Kalyanaraman**[2], and **Narayan G. Avadhani**[1,£]

[1]Department of Animal Biology, School of Veterinary Medicine, 3800 Spruce Street, University of Pennsylvania, Philadelphia, PA 19104, USA

[2]Department of Biophysics, Medical College of Wisconsin, 8701 Watertown Plank Road, Milwaukee, WI 53226.

Abstract

Cytochrome c Oxidase (CcO) is a multisubunit bigenomic protein complex which catalyzes the last step of the mitochondrial electron transport chain. The nuclear encoded subunits are thought to have roles either in regulation or in the structural stability of the enzyme. Subunit Vb is a peripheral nuclear-encoded subunit of mammalian CcO that is dramatically reduced under hypoxia. Although it has been shown to contain different ligand binding sites and undergo modifications, its precise function is not known. In the present study we generated a cell line from RAW 264.7 murine macrophages, that has more than 80% reduced level of Vb. Functional analysis of these cells showed a loss of CcO activity, membrane potential and lower ability to generate ATP. Resolution of complexes on Blue native gel and two dimensional electrophoretic analysis showed an accumulation of subcomplexes of CcO and also reduced association with super complexes of the electron transfer chain. Furthermore, the mitochondria from CcO Vb knock down cells generated increased ROS and the cells were unable to grow on galactose containing medium. Pulse chase experiments suggest the role of CcO Vb subunit in the assembly of the complex. We show for the first time the role of a peripheral, non-transmembrane subunit in the formation as well as function of the terminal CcO complex.

Introduction

Cytochrome c Oxidase (CcO) is the terminal enzyme of the mitochondrial electron transport chain, which catalyses the transfer of electrons from reduced Cytochrome c to molecular oxygen. The mammalian enzyme is composed of 13 subunits and is bi-genomic with subunits encoded by both mitochondrial DNA and the nuclear genome. MtDNA codes for the three largest subunits (CcO subunits I, II and III) that form the catalytic core of the enzyme. The remaining 10 subunits (in mammals, CcO IV, Va, Vb, VIa, VIb, VIc, VIIa, VIIb, VIIc, and VIII) are nuclear encoded, translated in the cytosol and imported into the mitochondria. During the catalytic cycle, reduced Cytochrome C binds to subunit II and transfers electrons to CuA

£ Address correspondence to: Narayan G. Avadhani (narayan@vet.upenn.edu; Fax: 215-573-6651).
*These two authors contributed equally to the paper.
Author contributions: DG and SS carried out most of the biochemical analysis and assisted in writing the paper. HR carried out the ROS assays and assisted in writing the paper. SKP prepared the stable expression cell line. MH, CK, ML and BK carried out the low temperature EPR and spin trapping assays. NGA was involved in the planning of the experiment, analysis of data and writing the paper.

site. Reduced CuA then transfers the electrons through heme a to heme a3/CuB binuclear reaction center, both associated with subunit I, where they are used to reduce molecular oxygen to water. Thus subunits I and II, by themselves carryout the complete redox cycle of cytochrome oxidase. The role of subunit III is not very well understood although it is believed to modulate proton pumping [1]. CcO from *Paracoccus* and *Thermus* contain only two subunits, that are homologous to subunits I and II of mammalian enzyme, and yet are catalytically similar to the mitochondrial enzyme [2]. However, human patients with deletions in subunit III exhibit cytochrome oxidase deficiency implying a possible role in the stability or assembly of the complex [3]. A single redox cycle of the enzyme is accompanied by the transport of two protons from the matrix to the inter membrane space, thus contributing to the transmembrane proton gradient and providing the free energy needed for ATP synthesis [4].

The nuclear subunits are small and surround the catalytic core of the enzyme [5]. Their number varies in different organisms. With the mitochondrial subunits harboring the reaction centers necessary for electron transport their role in the function of the enzyme are defined [1,6,7]. Since the bacterial enzyme with only the three catalytic subunits is functional, the precise roles of the nuclear subunits in the eukaryotic enzyme are not well understood. However, it is believed that they are involved in the regulation and assembly of the complex [5,8]. In *Saccharomyces cerevisiae* null mutants of IV, Va, VI, VII and VIIa lack CcO activity and fail to grow on nonfermentable carbon sources [8-10]. These subunits are thought to be involved in both stability and regulation of enzyme activity [11]. Loss of subunit VIII however, leads to only 20% decrease in enzyme activity and is required for formation of stable cytochrome oxidase dimers [11,12]. Using siRNA mediated mRNA depletion, the roles of the mammalian nuclear subunits are now being elucidated. In mouse fibroblast cells, stable siRNA depletion of CcO subunit IV caused a 70% reduction in CcO activity [13]. In contrast, removing CcO VIb from the purified bovine complex surprisingly resulted in substantially increased enzyme efficiency [14].

Crystal structure of beef heart CcO [15] shows that CcO Vb is an extra-membrane subunit located on the matrix side of the complex with its C-terminus in direct contact with CcO I and its N-terminus in direct contact with CcO II. The subunit contains a zinc binding site within the context of a zinc finger motif, though the physiological relevance of this is not known [15]. Unlike subunits IV, VIa, VIIa, and VIII, CcO Vb does not have any discrete developmental or tissue specific isoforms. However, previous work from our laboratory has shown that the subunit Vb content varies with tissue type [16] and even within different cardiac compartments of the heart [17]. In general, tissues with higher metabolic demands also exhibit the highest levels of CcO Vb, suggesting a role for CcO Vb in the function of the mammalian complex. In support of the essential role of CcO Vb in the regulation of the CcO activity, studies have demonstrated that the subunit is phosphorylated in a cAMP dependent manner [18]. Also, hypoxia has been shown to cause a decrease in CcO Vb protein level, which is accompanied by a decrease in enzyme activity [18-20]. Genetic studies in yeast have suggested role for the CcO IV subunit (homolog of mammalian Vb) in the stability of the complex [21-23]. Eaton and colleagues [24] have shown that transient siRNA depletion of CcO Vb resulted in decreased CcO activity and suggested a regulatory role for CcO Vb.

In light of the accumulating evidence that nuclear encoded subunits, particularly CcO Vb, are essential for the proper regulation and assembly of mammalian CcO, we generated a stable CcO Vb silenced murine macrophage RAW 264.7 cell line. The choice of this cell line was based on our previous study which showed that, these cells are highly sensitive to hypoxia and CcO activity as well as subunit Vb levels were reduced under hypoxic condition [18]. The CcO Vb silenced cell line exhibited dramatically reduced CcO activity and an inability to form functional complexes, which was accompanied by a drastic reduction in respiration, lower membrane potential and increased reactive oxygen species formation. Collectively, our data

suggest that CcO Vb is essential for the assembly and stability of a functional CcO complex. To date, this is the first report on the requirement for a non-transmembrane spanning peripheral nuclear subunit in the assembly and stability of the mammalian cytochrome oxidase.

Materials and Methods

Generation of CcO Vb Depleted RAW 264.7 Cells

The mouse CcO Vb mRNA transcript (NM_009942) was analyzed for siRNA target regions using the siRNA algorithm on the Dharmacon website (http://www.dharmacon.com/sidesign/designresults.aspx). The target region with the highest score was 5'-GAGGACAACTGTACTGTCA-3'. A siRNA oligonucleotide specific for this sequence was synthesized and cloned into the pSilencer 2.0 vector according to the manufacturer's protocol (Ambion). A target sequence with no significant homology to any mouse transcript was also cloned and used as a control. RAW 264.7 macrophages (ATCC# TIB-71) were maintained in DMEM (Invitrogen) supplemented with 10% FBS (Atlanta Biologicals) and 0.1% gentamicin (Invitrogen). Cells were grown to 60% confluence in 6-well plates and 2 μg of pSilencer plasmid per well (containing either CcO Vb or control siRNA) was transfected using Targefect-RAW according to the manufacturer's instructions (Targeting Systems Santee, CA). The cells were switched to selection media containing 250 μg/ml Geneticin (Invitrogen), 48 hours after transfection, and maintained for two weeks with media changes every three to four days. Selected colonies were analyzed for CcO Vb levels by both real time PCR and western blotting.

Quantitative Real Time PCR

Total RNA was isolated from individual clones using Trizol reagent (Invitrogen) and stored at −80° C. For real time PCR analysis, cDNA was synthesized using the High Capacity cDNA Archive Kit (Applied Biosystems). Relative mRNA levels of subunits CcO I, CcO II, CcO IV or CcO Vb subunits were determined by standard SYBR Green real time PCR reactions on an ABI 7300 Real Time PCR Machine. The levels of the various CcO transcripts were normalized to β-Actin and expressed as the fold change compared to the value obtained for the clone transfected with the non-specific siRNA (control).

Preparation of Mitochondrial and Whole Cell Extracts

Whole cell extract was prepared by lysing cells in 400 μl RIPA buffer (50 mM Tris-HCl pH 7.4, 1% NP-40, 0.25% sodium deoxycholate, 150 mM NaCl, 1 mM EDTA) containing Complete Protease Inhibitor Cocktail (Roche). The crude lysate was sonicated, incubated at 4°C for 1 hour and centrifuged. Protein concentration of the supernatant was estimated by the method of Lowry and aliquots were stored at −80°C until use.

Mitochondria were prepared by differential centrifugation as described before [18]. Briefly, cells were washed with cold PBS and homogenized with a Dounce glass homogenizer in H-medium (70 mM sucrose, 220 mM mannitol, 2.5 mM HEPES pH 7.4, 2 mM EDTA, Complete Protease Inhibitor Cocktail). Subcellular fractions were prepared by differential centrifugation. Protein concentration of the final mitochondrial suspension was performed according to the method of Lowry and aliquots were stored at −80°C until use.

SDS and Blue Native PAGE

For SDS-PAGE analysis, either 40 μg of mitochondrial extract or 80 μg of whole cell extract was separated on a 12% denaturing polyacrylamide gel. Protein was then transferred to nitrocellulose membranes (BioRad) and stored dry between filter paper until use.

Blue Native PAGE was carried out essentially as described before [25]. Briefly, 150 μg of mitochondria was solubilized in 30 μl of solubilization buffer containing 1.5 M aminocaproic acid, 50 mM Bis-Tris and 0.2% dodecyl maltoside and incubated on ice for 30 minutes. The insoluble material was pelleted by centrifugation at 100,000 × g for 30 minutes and the supernatant was mixed with Blue Native loading buffer (750 mM aminocaproic acid, 50 mM Bis-Tris, 0.5 mM EDTA, 5% Serva Blue G) and separated on either a 5-16% (when probed for CcO or Complex II) or a 5-13% native gradient gel (when probed for Complex I, III or V). The gels were run at 100 V, initially with cathode buffer containing the blue dye. When the dye front reached the middle of the gel the buffer was replaced by clear cathode buffer. Electrophoresis was carried out till the blue dye reached the end of the gel. Protein was transferred to PVDF membrane (20mA, 30 min) and used for immunoblotting.

Two dimensional blue native/SDS PAGE gel analysis for detection of subcomplexes and supercomplexes of electron transport chain

In the first dimension, the electron transport chain complexes were separated by blue native PAGE as described above. 5-13% gradient acrylamide gel was used for resolving intact complexes by Blue Native Gel analysis, and 8-16% gradient was run for resolving subcomplexes of CcO. For the second dimension analysis, individual lanes from first dimension were excised and incubated for one hour in a denaturing solution containing 1% SDS and 1% 2-mercaptoethanol. The gel strip was placed at 90° from its original orientation in the stacking gel area of a 10% Tricine SDS acrylamide gel as described by Nijtmans [25] and standard SDS-PAGE was performed. At the completion of the second dimension run, protein was transferred to Immunoblot PVDF membrane and probed with antibodies specific for CcO subunit I.

Metabolic labeling to follow CcO assembly

The metabolic labeling and analysis of labeled complex IV was carried out using a method modified from Nijtmans et al [25]. Control and VbKD RAW 264.7 cells were grown to 60% confluence in complete DMEM medium with 10% FBS. The cells were treated with 30 μg/ml of cycloheximide in Cysteine/Methionine free DMEM medium for 1h. At the end of incubation, 20 μCi of S^{35}-Methionine was added per ml of medium. After 2h of incubation, the radioactive label was chased with regular DMEM medium without cycloheximide for 3h. Mitochondria were isolated and the electron transport chain proteins were separated by two dimensional 8-15% blue native/ Tricine SDS PAGE as described before. After separation, the gels were dried and the radio labeled proteins were analysed by autoradiography.

Immunoblot Analysis

Antibodies specific for NDUFA9 (subunit of Complex I), Core 1 (subunit of complex III), ATPase Subunit β (subunit of Complex V), CcO I, CcO IV, CcO Va, CcO Vb (Mitoscience), 70kDa subunit of Complex II (Molecular Probes), TOM 20 (Santa Cruz), and β-Actin (Santa Cruz) were diluted 1:5000; the monoclonal antibody specific for CcO II (Santa Cruz) was diluted 1:2000. Blots were probed and developed using the Super Signal West Femto System (Pierce) and imaged on a BioRad VersaDoc Imaging system. Digital image analysis was performed using Quantity One v4.5. The density of each band was then normalized to the loading control (either TOM 20 or β-actin), and the fold change was calculated and compared to the control extract.

OXPHOS Complex Assays and Oxygen Consumption

Assays for Complex I, Complex II-III and CcO were essentially as described by Birch-Machin and Turnbull [26] using a Cary 1E UV-Vis Spectrophotometer. Briefly, Complex I activity (NADH: ubiquinone oxidoreductase) was measured by incubating 50 μg of freeze thawed

mitochondrial extract in 1 ml of assay medium (25 mM potassium phosphate pH 7.4, 5 mM $MgCl_2$, 2mM NaCN, 2.5 mg/ml BSA, 13 mM NADH, 65 μM ubiquinone, 2 μg/ml Antimycin A) and measuring the decrease in absorbance at 340 nm due to NADH oxidation. Complex II-III activity (succinate-Cytochrome C reductase) was measured by incubating 20 μg of freeze thawed mitochondrial extract in 1 ml of assay medium (25 mM potassium phosphate pH 7.4, 2 mM NaCN, 20 mM succinate, 2 μg/ml rotenone, 37.5 μM oxidized Cytochrome C) and measuring the increase in absorbance at 550 nm due to Cytochrome C reduction. CcO activity (Cytochrome C oxidase) was measured by incubating 5 μg of freeze thawed mitochondrial extract in 1 ml of assay medium (25 mM potassium phosphate pH7.4, 0.45 mM dodecyl maltoside, 15 mM reduced Cytochrome C) and measuring the decrease in absorbance at 550 nm due to Cytochrome C oxidation. Oxygen consumption was measured using a Strathkelvin Model 781 Oxygen Sensor by incubating 100 μg of mitochondrial extract in 1 ml of 25 mM potassium phosphate pH 7.4 containing 40 mM succinate and 15 μM reduced Cytochrome C and following the decrease in oxygen content of the closed system.

Measurement of mitochondrial membrane potential and cellular ATP Levels

The membrane potential was measured as a function of mitochondrial uptake of MitoTracker Orange CM-H2TM ROS (50 nM) added to the cell suspension. Fluorescence was monitored in a multiwavelength-excitation dual wavelength-emission Delta RAM PTI spectrofluorometer at 525 nm Excitation and 575 nm Emission [27]. Total cellular ATP levels were determined by bioluminescence using ATP-bioluminescent somatic cell assay kit (Sigma) following the manufacturers instructions. Briefly, 10^6 cells were lysed using the “somatic cell releasing reagent,” which caused the release of cellular ATP by altering membrane permeability. ATP-dependent formation of light was measured in a TD-20/20, Turner designs luminometer. The relative intensity was calculated.

Heme Content Analysis

900 μg of freeze thawed mitochondrial extract was incubated on ice for 30 minutes in 2 ml of 25 mM phosphate buffer pH 7.4 containing 2% dodecyl maltoside before being split into two cuvettes. About 10-20 μg of sodium ascorbate were added to one of the cuvettes and the reduced minus oxidized difference spectra was recorded from 400 nm to 800 nm after incubation for 10 min at room temperature.

Low temperature EPR of whole cells

Control and VbKD (Vb mRNA knocked down) cells were harvested and washed once with PBS. The cell pellet was resuspended in 200 μl of H-medium and transferred into 4-mm quartz EPR tubes (Wilmad Glass, Buena, NJ) and the sample was frozen in liquid nitrogen and stored at −70 °C until EPR measurements were performed. The X-band EPR of the whole cells were recorded at liquid helium temperatures on a Bruker E500 ELEXYS spectrometer with 100 kHz field modulation, equipped with an Oxford Instrument ESR-9 helium flow cryostat and a DM-0101 cavity. Spectrometer conditions were as follows: microwave frequency, 9.635 GHz; modulation frequency, 100 kHz; modulation amplitude, 10 G; receiver gain, 85 dB; time constant, 0.01 s; conversion time, 0.08 s; sweep time, 83.9 s. EPR spectra were obtained over the temperature range 4-50 K using an incident microwave power of 5 mW and modulation amplitude of 10 G. The spectrometer was calibrated with the radical 1, 1-diphenyl-2-picrylhydrazyl (DPPH) exhibiting an EPR signal centered at g = 2.0036.

Growth Curve

Cells were grown to ~70% confluence in 100 mm dishes without selection and viable cells were counted using trypan blue exclusion. 3×10^5 cells were then plated in 6 well dishes containing 3 ml culture medium and the number of viable cells per well was determined every

12 hours or 24 hours. To measure the ability of the cells to grow in presence of non-fermentable carbon source, the medium was replaced with glucose free medium containing 0.9 mg/ml galactose, 0.5mg/ml pyruvate and 10% dialyzed FBS.

Detection of reactive oxygen species

Dichlorofluorescein fluorescence—ROS formation was measured by DCFHDA oxidation by a modified method of LeBel et al [28]. Mitochondria (50 μg) from control and Vb knockdown cells were incubated with DCFHDA. DCFH is oxidized by reactive oxygen intermediates to a fluorescent compound which is measured at 525nm after excitation at 488nm. Fluorescence was measured continuously for 15 minutes.

EPR Measurements—Mitochondria targeted spin trap, MitoDEPMPO was used to detect reactive oxygen radicals in intact mitochondria. MitoDEPMPO was synthesized by covalently linking DEPMPO to tryphenylphosphonium ion according to the method described in Hardy et al [29]. Reaction mixtures for EPR were prepared in phosphate buffered saline (pH 7.3) containing 1mM DTPA and MitoDEPMPO (100mM) in a final volume of 50μl. The electron transport chain was initiated by adding succinate (10 μM) and the EPR spectrum was recorded at 37°C using a Bruker EMX spectrometer at 9.5 GHz (X-band) employing a 100 kHz field modulation. When using DEPMPO as the spin trap, the mitochondria were first solubilized with 0.5% dodecyl maltoside before adding the trap. The EPR parameters for all experiments were as follows: Microwave power; 20 mW; modulation amplitude, 1 G; time constant, 1.28 ms; gain 10^6; sweep time, 335.54; conversion time, 0.163 s, 4 scans.

Statistical analysis—Activity data is presented as mean ± SE of mean. EPR traces shown in the figure are the summation of three scans.

Results

Stable knockdown of Cytochrome c Oxidase subunit Vb

Three different siRNA target regions were identified in the CcO Vb transcript. Transient transfections showed siRNA 5’ GAG GAC AAC TGT ACT GTC A 3’ was most effective in silencing CcO Vb expression in RAW 264.7 cells. Clones stably expressing this siRNA were screened for Vb protein levels. Figure 1A and 1B show that clone 1 (VbKD1) had only 15% residual CcO Vb protein and 23% residual CcO Vb mRNA. This clone was used in all subsequent experiments as the CcO Vb silenced cell line (VbKD). In all experiments in this study the control is RAW 264.7 cell line stably transfected with a scrambled siRNA sequence not specific for any mouse transcript (Figure 1A and 1B).

Effect of Vb silencing on Cytochrome oxidase level and function

Subunit Vb has no known function in cytochrome oxidase activity. To determine the effect of absence of Vb on CcO, we measured both the protein level and activity of cytochrome oxidase in VbKD cells. Figures 1C and 1D show that mitochondria from VbKD cells had only 20-22% residual CcO activity measured by rate of oxygen consumption and oxidation of reduced cytochrome C, respectively compared to control mitochondria. The activity measured was specific as observed by inhibition by potassium cyanide (data not shown).

To determine if the loss of CcO activity was due to a decrease in the holoenzyme we performed blue native gel analysis of mitochondria from control and VbKD cells. Figure 2A shows the blue native gel pattern of complexes from control and VbKD cells. The intensity of stained CcO complex was markedly lower in the knock down cells than in control cells. Figure 2B shows the immunoblot of companion gels developed using antibodies against both mitochondrial DNA encoded (subunits I and II) and nuclear gene encoded (subunits IV, Va

and Vb) subunits of CcO. We were unable to detect any intact CcO complex containing CcO I, CcO II, CcO IV or CcO Va in VbKD mitochondria (Figure 2B). Complex II, which was not affected by Vb knockdown, was used as control. Since electrophoretic transfer of 200 kDa protein complexes is not quantitative we wanted to confirm the observed lack of CcO by analyzing heme a/a3 content, which is a cytochrome exclusive to CcO. Accordingly, the reduced minus oxidized difference spectra shows that the heme a/a3 level was reduced by 71.4%, while the heme c/c1 peak, a component of Complex III, remained unchanged (Figure 2C). This is consistent with the observed reduction in cytochrome oxidase activity in VbKD mitochondria. Studies [30,31] have shown that low temperature EPR spectroscopy can be used to detect the redox states of heme, Cu and Fe/S centers associated with mitochondrial complexes I, II, III and IV in heart and other tissues. EPR spectra of control and VbKD cells show marked difference in low spin heme a (g=3) and heme a3/CuB of CcO (g=2.95, g=12). Results show selective loss of exchange coupled resonances at g=2.95 and g=12, confirming a marked change in the CcO complex in VbKD cells (Figure 2E) but no significant change in Fe/S clusters (Figure 2D) of other complexes.

Since CcO is a multisubunit protein, we determined the levels of some of the other subunits of CcO in the mitochondrial extract. As shown in Figure 3A, the levels of CcO I, CcO II, CcO IV and CcO Va were all reduced to varying levels in response to CcO Vb depletion. To understand the basis of reduction in subunit levels we evaluated the levels in whole cell extract (Figure 3B) which was nearly comparable to the level in mitochondrial extracts. However, the mRNA levels of CcO I, CcO II and CcO IV were increased to a small extent (Figure 3E), suggesting either increased expression or increased mRNA stability. This suggests that the reduction in subunit levels was not due to reduced transcription but more likely due to the rapid degradation of unassembled subunits.

Defective Cytochrome oxidase assembly in Vb knockdown cells

In order to understand the loss of other subunits of CcO in VbKD cells, we investigated the rate of assembly of cytochrome oxidase complex. Pulse chase analysis was done by selective labeling of mitochondrial subunits with S^{35} Methionine/Cysteine in presence of cycloheximide, an inhibitor of cytosolic protein synthesis. Cytochrome oxidase assembly was then allowed to continue in the absence of cycloheximide and with unlabeled Methionine/Cysteine. Figure 4A shows the autoradiograph of BN PAGE/Tricine SDS two dimensional gel of mitochondria isolated from control and VbKD cells after pulse chase. The blue native gel conditions (8-15%) was such that only complexes II and IV entered the gel. The larger complexes (I, III and V) remained at the top of the gel. Also since complex II does not contain any mitochondrial encoded subunits, this method allowed us to selectively view the labeling of complex IV. An SDS PAGE pattern of CcO I is shown in Figure 4A and the quantitation of the blot in Figure 4B. Results show that a total of 64% of the labeled protein was associated with the holoenzyme complex plus the S3 subcomplex in control cells compared to only 25% in VbKD mitochondria (Figure 4B). However, in VbKD cells about 54% of the total label is associated with subcomplex S1 compared to only 25.4% in control cells. Likewise, in VbKD cells subcomplex S2 constituted 21.7% of the label compared to 9.7% in control cells. To confirm that these are indeed subcomplexes of cytochrome oxidase, we performed western blot analysis on ETC complex proteins separated on 2D BN PAGE/Tricine SDS gels. The SDS gel resolved complexes were probed with CcO subunit I antibody. As seen from immunoblot in Figure 4C and quantitation in Figure 4D there is a clear accumulation of CcO subunit I-containing smaller complexes in mitochondria of VbKD cells compared to control cells. Collectively, the reduced level of the 200 kDa CcO monomer, the reduced heme a/a3 content and the higher levels of CcO I subunit containing subcomplexes demonstrate that CcO assembly is disrupted and the CcO level is significantly reduced in RAW 264.7 cells lacking

subunit Vb. Additionally, the higher order of complexes designated as supercomplexes observed in control cell mitochondria are decreased in mitochondria from VbKD cells.

Effect of Vb silencing on mitochondrial functions

A previous study has shown that CcO stability is required for Complex I formation in mouse embryonic fibroblasts [13]. In an effort to determine if the loss of CcO activity due to the silencing of Vb affects other ETC complexes, we analyzed the protein levels and functions of the remaining complexes in CcO Vb deficient macrophages. Interestingly, there was no difference in the protein levels of complexes I, II, III and V (Figure 2B and 5A). Similarly the activities of complex I, II/III (Figure 5B) were not significantly affected in VbKD mitochondria. The respiratory chain enzymes are known to be organized into multienzyme structures called supercomplexes. Western blot analysis of complexes from control cell and VbKD cell mitochondria resolved on 2D BN PAGE/Tricine gel (Figure 5C) shows a loss of supercomplexes in VbKD cells. We assayed the VbKD cells for total cellular ATP and membrane potential. Silencing CcO Vb mRNA reduced total cellular ATP by 38% (Figure 6A) and significantly decreased mitochondrial membrane potential, as evidenced by a reduction in the ability to sequester MitoTracker Orange (Figure 6B).

As expected for a cell line deficient in CcO, we observed that the VbKD cells had retarded growth rate. The altered growth was apparent 24 hours after plating 50,000 viable control and VbKD cells and grew in disparity over the next 48 hours (Figure 6C). After 72 hours, there were 57% fewer viable VbKD cells than Control. To assess the extent of mitochondrial dysfunction, control and VbKD cells were grown in medium containing galactose, a non fermentable sugar, instead of glucose. As seen from the graph (Figure 6D), only 10% of VbKD cells survived after 6 days compared to control cells.

Increased reactive oxygen species formation in Vb knockdown cells

Defective electron transport chain is a common cause for increased reactive oxygen species (ROS) formation in the mitochondria. Since CcO Vb silencing affects many of the mitochondrial functions, it seemed likely that cells lacking CcO Vb may produce more ROS. We assayed the extent of ROS production using two different approaches. In the first method, we measured cellular ROS production fluorometrically using DCFDA. Briefly, non-fluorescent DCFDA is freely taken up by respiring cells and is cleaved into DCFH by intracellular esterases [32]. The probe is oxidized by hydrogen peroxide radicals to a highly fluorescent compound. Figure 7A shows a steady increase in the DCF fluorescence in the cells with time. VbKD cells produced ~60% higher fluorescence than control cells indicating increased ROS production. Azide, a specific inhibitor of CcO activity also induced a similar increase in ROS production. Addition of antioxidant N-Acetyl cysteine, vastly reduced the fluorescent signal suggesting the specificity of this assay system. To confirm the mitochondrial origin of ROS, we used EPR spin trapping with a mitochondria targeted probe MitoDEPMPO that was recently reported by us [29]. Isolated mitochondria were loaded with mitoDEPMPO and the electron transport was initiated by adding succinate. Mitochondria from VbKD cells yielded an EPR spectrum with a three fold higher level of superoxide, hydroxyl and alkyl adducts compared to control mitochondria (Figure 7B). To confirm the intramitochondrial origin of the signal, mitochondria were separately incubated with DEPMPO, which does not enter intact mitochondria. As seen in Figure 7B, the signal from DEPMPO was basal. However, solubilizing the mitochondria with dodecyl maltoside before incubating with DEPMPO resulted in a significant increase in spin adducts. Figure 7C shows the structure of hydrogen peroxide conjugated mitoDEPMPO. These results show that loss of cytochrome oxidase activity due to CcO Vb knockdown causes increased production of reactive oxygen species.

DISCUSSION

It is now well established that CcO represents an important site of regulation of mitochondrial oxidative phosphorylation and ATP generation. A number of human diseases are linked to CcO deficiency or dysfunction [33-35]. CcO activity is known to be regulated by an array of factors including allosteric modulators, protein modification, mutations in both mitochondrial and nuclear genes and physiological factors such as hormones [36-40]. Although the functions of mitochondrial encoded subunits in mammalian organisms have been well established, relatively less is known about the role of nuclear encoded subunits in the assembly, structural integrity or activity of the mammalian complex [8]. It is generally assumed that the nuclear subunits have a role in the regulation, or in binding physiological modulators [8,20]. In this paper we provide a direct and unequivocal evidence for the role of CcO Vb in the assembly of the mouse CcO complex in the Vb mRNA silenced RAW 264.7 cells.

Previously we have shown that different tissues with different oxidative capacity such as liver and heart show varying levels of CcO Vb contents in relation their heme aa3 contents [17]. Similarly, different compartments of the heart exhibiting different O_2 loads also showed a difference in CcO Vb contents [17]. More recently using a Langendorf perfusion system we showed that CcO Vb levels declined in rabbit hearts subjected to ischemia/reperfusion, in relation to their heme aa3 contents, suggesting preferential loss of some of the peripheral subunits from the holoenzyme complex which was also accompanied by a loss of CcO activity [18]. Similarly, RAW 246.7 macrophages exposed to hypoxia also show selective decrease of subunits IVi1 and Vb and associated loss of CcO activity [18]. Proteomic studies on mitochondria from cancer patients with reduced CcO activity also showed a reduction in CcO Vb subunit contents [41].

In this study we sought direct evidence on the role of subunit Vb in CcO function/activity by generating RAW 264.7 macrophage cell line stably expressing siRNA to Vb mRNA. The cell line used in this study contains ~80% reduced Vb mRNA and subunit levels. Remarkably, VbKD cells showed markedly reduced holoenzyme complex, reduced bimolecular EPR signal suggesting an altered enzyme, a markedly increased level of subcomplexes, reduced heme aa3 content, disruption of $\Delta\Psi m$, and vastly reduced CcO activity. Crystal structure of bovine CcO complex revealed that Vb subunit is a peripherally associated with CcO facing the matrix side of the complex [15]. This raises the question on the role of CcO Vb either in the stability of the enzyme complex or in its assembly. Results on pulse-chase analysis of CcO in control and VbKD cells (Figure 4A) clearly suggest the latter. Using transient siRNA transfection Campian et al., [24] showed a reduction in CcO activity and ~20% reduction in CcO II. A marginal effect on the steady state level of other subunits in this study likely reflects a marginal depletion of Vb mRNA by the transient transfection method used [24].

Interestingly, SDS PAGE analysis of both mitochondrial and whole cell extracts also showed a similar decrease in other subunits of CcO in VbKD cells. However, real-time quantitation of mRNA levels showed a small but significant increase in the steady state levels of these mRNAs. We believe that this increase is reminiscent of compensatory increases of mRNAs for mitochondrial energy transducing complexes and other proteins known to occur in cells with dysfunctional mitochondria [42-44]. We also believe that reduced subunit level probably reflects rapid degradation of unassembled subunits in the matrix or in the cytoplasm. Extensive studies in yeast have shown that the assembly of CcO is a highly organized sequential process [25]. Yeast strain with deleted subunit IV, the yeast homolog of mammalian subunit Vb, failed to assemble intact CcO complex [22,23]. Similarly, mutations at the zinc finger domain of yeast CcO IV (homolog of mammalian Vb) severely affected CcO activity [21]. These genetic data support our present observations on loss of CcO activity and loss of a number of other subunits in VbKD cells. Notably, knock down of Vb in our study caused reduction in the steady

state levels of nuclear subunits IV and Va. In the yeast system however, knock down of CcO IV (homolog of mammalian Vb) only marginally reduced the steady state levels of nuclear subunits CcO Va/b (mammalian CcO IV) and CcO VI (mammalian CcO Va) [22,23]. The reasons for this difference remain unclear.

Recently it was shown that a functional assembled CcO is necessary for the stability of complex I [13]. Loss of CcO in knockout mice lacking CcO subunit 10, a CcO assembly factor, also resulted in the loss of complex I [45]. The prevailing hypothesis is that presence of CcO in proper abundance is needed for the formation of respirasome [46,47], the supercomplexes containing one or more copies of complexes I, III and IV. This arrangement is thought to increase the efficiency of electron transfer and minimizes the leakage of electrons that can potentially generate reactive oxygen radicals [46-48]. In VbKD cells, however, despite a marked reduction in CcO complex and the supercomplex structures, we have observed no decrease in the content or activity of complex I. It is likely that CcO subunit 10, a known chaperone plays a direct or indirect role in the assembly of complex I as well. Further studies are therefore necessary to understand the role of CcO complex in the stability of complex I.

An important observation was the formation of mitochondrial ROS in VbKD cells. Mitochondrial electron transport chain is an important source of reactive oxygen species in respiring cells. Among the mitochondrial sites, complex I and III are considered as significant sources of ROS [49-51]. ROS formation by complex I is thought to be due to the reverse flow of electrons under limiting substrate conditions. This is a common phenomenon during hypoxia where complex I is considered the major source of ROS. Also, ROS generated by this site may or may not depend on mitochondrial membrane potential depending on the substrate oxidized and the activities of the other energy transducing complexes [52]. Complex III is another known site of superoxide formation where auto oxidation of accumulated semiubiquinone anion radical has been implicated and ROS production at this site depends on $\Delta\Psi m$ [52]. To confirm the mitochondrial origin of ROS, we used a mitochondria targeted EPR spin trap, mitoDEPMPO [29]. We found a significantly higher level of both hydroxyl and superoxide radicals in VbKD cells compared to control cells. Since CcO is not known to be a site of ROS production, the origin of these reactive species in VbKD cells needs to be established. It is possible that blocking of electron transport chain in these cells leads to the accumulation of reduced semiubiquinone, which in turn may be the cause of ROS. However, a disrupted $\Delta\Psi m$ in these cells is unlikely to support this reaction mechanism. Another possibility is the abnormal subcomplexes of CcO accumulated in the mitochondrial membrane in VbKD cells. Recently Khalimonchuk et al., [53] showed in yeast that CcO subunit I-heme a, is a pro-oxidant intermediate formed during the assembly of cytochrome oxidase. Thus, assembly defective complexes of CcO in VbKD cells may be another source of reactive oxygen species.

In summary, in line with studies on subunit IVi1 and VIaH depletion reported recently [54, 55], our results show that the nuclear encoded peripheral subunit Vb plays a direct role in the assembly and activity of mammalian CcO complex. These results also suggest that subunit IVi1 and Vb, in particular may have a more direct role in the assembly or integrity of the complex rather than their previously predicted role in the regulation of enzyme activity. This is also the first demonstration of a structural role for a peripheral, non-integral membrane subunit of mammalian cytochrome oxidase.

Acknowledgement

We are thankful to various colleagues from the Avadhani and Kalyanaraman laboratories for useful discussion and suggestions. This research was supported in part by NIH grants GM-49683 and AA-017749.

Abbreviations

CcO, Cytochrome C Oxidase; VbKD, subunit Vb silenced cells; PAGE, Polyacrylamide gel electrophoresis; BNGE, blue native gel electrophoresis; SDS, sodium dodecyl sulphate; ROS, reactive oxygen species; EPR, electron paramagnetic resonance; DCFHDA, dichlorofluorescein diacetate.

References

1. Brunori M, Antonini G, Malatesta F, Sarti P, Wilson MT. Cytochrome-c oxidase. Subunit structure and proton pumping. Eur.J.Biochem 1987;169:1–8. [PubMed: 2445564]
2. Dowhan W, Bibus CR, Schatz G. The cytoplasmically-made subunit IV is necessary for assembly of cytochrome c oxidase in yeast. EMBO J 1985;4:179–184. [PubMed: 2990892]
3. Keightley JA, Hoffbuhr KC, Burton MD, Salas VM, Johnston WS, Penn AM, Buist NR, Kennaway NG. A microdeletion in cytochrome c oxidase (COX) subunit III associated with COX deficiency and recurrent myoglobinuria. Nat.Genet 1996;12:410–416. [PubMed: 8630495]
4. Wikstrom MK. Proton pump coupled to cytochrome c oxidase in mitochondria. Nature 1977;266:271–273. [PubMed: 15223]
5. Capaldi RA. Structure and function of cytochrome c oxidase. Annu.Rev.Biochem 1990;59:569–596. [PubMed: 2165384]
6. Babcock GT, Wikstrom M. Oxygen activation and the conservation of energy in cell respiration. Nature 1992;356:301–309. [PubMed: 1312679]
7. Cooper CE, Nicholls P, Freedman JA. Cytochrome c oxidase: structure, function, and membrane topology of the polypeptide subunits. Biochem.Cell Biol 1991;69:586–607. [PubMed: 1665335]
8. Poyton RO, McEwen JE. Crosstalk between nuclear and mitochondrial genomes. Annu.Rev.Biochem 1996;65:563–607. [PubMed: 8811190]
9. Aggeler R, Capaldi RA. Yeast cytochrome c oxidase subunit VII is essential for assembly of an active enzyme. Cloning, sequencing, and characterization of the nuclear-encoded gene. J.Biol.Chem 1990;265:16389–16393. [PubMed: 2168889]
10. Calder KM, McEwen JE. Deletion of the COX7 gene in Saccharomyces cerevisiae reveals a role for cytochrome c oxidase subunit VII in assembly of remaining subunits. Mol.Microbiol 1991;5:1769–1777. [PubMed: 1658541]
11. Poyton RO, Goehring B, Droste M, Sevarino KA, Allen LA, Zhao XJ. Cytochrome-c oxidase from Saccharomyces cerevisiae. Methods Enzymol 1995;260:97–116. [PubMed: 8592475]
12. Patterson TE, Poyton RO. COX8, the structural gene for yeast cytochrome c oxidase subunit VIII. DNA sequence and gene disruption indicate that subunit VIII is required for maximal levels of cellular respiration and is derived from a precursor which is extended at both its NH2 and COOH termini. J.Biol.Chem 1986;261:17192–17197. [PubMed: 3023386]
13. Li Y, D'Aurelio M, Deng JH, Park JS, Manfredi G, Hu P, Lu J, Bai Y. An assembled complex IV maintains the stability and activity of complex I in mammalian mitochondria. J.Biol.Chem 2007;282:17557–17562. [PubMed: 17452320]
14. Weishaupt A, Kadenbach B. Selective removal of subunit VIb increases the activity of cytochrome c oxidase. Biochemistry 1992;31:11477–11481. [PubMed: 1332762]
15. Tsukihara T, Aoyama H, Yamashita E, Tomizaki T, Yamaguchi H, Shinzawa-Itoh K, Nakashima R, Yaono R, Yoshikawa S. The whole structure of the 13-subunit oxidized cytochrome c oxidase at 2.8 A. Science 1996;272:1136–1144. [PubMed: 8638158]
16. Basu A, Lenka N, Mullick J, Avadhani NG. Regulation of murine cytochrome oxidase Vb gene expression in different tissues and during myogenesis. Role of a YY-1 factor-binding negative enhancer. J.Biol.Chem 1997;272:5899–5908. [PubMed: 9038208]
17. Vijayasarathy C, Biunno I, Lenka N, Yang M, Basu A, Hall IP, Avadhani NG. Variations in the subunit content and catalytic activity of the cytochrome c oxidase complex from different tissues and different cardiac compartments. Biochim.Biophys.Acta 1998;1371:71–82. [PubMed: 9565657]

18. Prabu SK, Anandatheerthavarada HK, Raza H, Srinivasan S, Spear JF, Avadhani NG. Protein kinase A-mediated phosphorylation modulates cytochrome c oxidase function and augments hypoxia and myocardial ischemia-related injury. J Biol Chem 2006;281:2061–2070. [PubMed: 16303765]
19. Fang JK, Prabu SK, Sepuri NB, Raza H, Anandatheerthavarada HK, Galati D, Spear J, Avadhani NG. Site specific phosphorylation of cytochrome c oxidase subunits I, IVi1 and Vb in rabbit hearts subjected to ischemia/reperfusion. FEBS Letters 2007;581:1302–1310. [PubMed: 17349628]
20. Kadenbach B, Huttemann M, Arnold S, Lee I, Bender E. Mitochondrial energy metabolism is regulated via nuclear-coded subunits of cytochrome c oxidase. Free Radic.Biol.Med 2000;29:211–221. [PubMed: 11035249]
21. Coyne HJ III, Ciofi-Baffoni S, Banci L, Bertini I, Zhang L, George GN, Winge DR. The characterization and role of zinc binding in yeast Cox4. J.Biol.Chem 2007;282:8926–8934. [PubMed: 17215247]
22. Glerum DM, Tzagoloff A. Submitochondrial distributions and stabilities of subunits 4, 5, and 6 of yeast cytochrome oxidase in assembly defective mutants. FEBS Lett 1997;412:410–414. [PubMed: 9276437]
23. McEwen JE, Ko C, Kloeckner-Gruissem B, Poyton RO. Nuclear functions required for cytochrome c oxidase biogenesis in Saccharomyces cerevisiae. Characterization of mutants in 34 complementation groups. J.Biol.Chem 1986;261:11872–11879. [PubMed: 3017950]
24. Campian JL, Gao X, Qian M, Eaton JW. Cytochrome C oxidase activity and oxygen tolerance. J.Biol.Chem 2007;282:12430–12438. [PubMed: 17303578]
25. Nijtmans LG, Taanman JW, Muijsers AO, Speijer D, Van den BC. Assembly of cytochrome-c oxidase in cultured human cells. Eur.J.Biochem 1998;254:389–394. [PubMed: 9660196]
26. Birch-Machin MA, Turnbull DM. Assaying mitochondrial respiratory complex activity in mitochondria isolated from human cells and tissues. Methods Cell Biol 2001;65:97–117. [PubMed: 11381612]
27. Buckman JF, Hernandez H, Kress GJ, Votyakova TV, Pal S, Reynolds IJ. MitoTracker labeling in primary neuronal and astrocytic cultures: influence of mitochondrial membrane potential and oxidants. J.Neurosci.Methods 2001;104:165–176. [PubMed: 11164242]
28. LeBel CP, Ali SF, McKee M, Bondy SC. Organometal-induced increases in oxygen reactive species: the potential of 2',7'-dichlorofluorescin diacetate as an index of neurotoxic damage. Toxicol.Appl.Pharmacol 1990;104:17–24. [PubMed: 2163122]
29. Hardy M, Rockenbauer A, Vasquez-Vivar J, Felix C, Lopez M, Srinivasan S, Avadhani N, Tordo P, Kalyanaraman B. Detection, characterization, and decay kinetics of ROS and thiyl adducts of mito-DEPMPO spin trap. Chem.Res.Toxicol 2007;20:1053–1060. [PubMed: 17559235]
30. Hagen WR, Dunham WR, Sands RH, Shaw RW, Beinert H. Dual-mode EPR spectrometry of O2-pulsed cytochrome c oxidase. Biochim.Biophys.Acta 1984;765:399–402. [PubMed: 6329275]
31. Cooper CE, Salerno JC. Characterization of a novel g' = 2.95 EPR signal from the binuclear center of mitochondrial cytochrome c oxidase. J.Biol.Chem 1992;267:280–285. [PubMed: 1309737]
32. Gomes A, Fernandes E, Lima JLFC. Fluorescence probes used for detection of reactive oxygen species. Journal of Biochemical and Biophysical Methods 2005;65:45–80. [PubMed: 16297980]
33. Cifelli PM, Hargreaves I, Grunewald S. Cytochrome oxidase deficiency in Lowe syndrome. J.Inherit.Metab Dis 2002;25:411–412. [PubMed: 12408191]
34. Robinson BH. Human cytochrome oxidase deficiency. Pediatr.Res 2000;48:581–585. [PubMed: 11044474]
35. DiMauro S, Zeviani M, Servidei S, Bonilla E, Miranda AF, Prelle A, Schon EA. Cytochrome oxidase deficiency: clinical and biochemical heterogeneity. Ann.N.Y.Acad.Sci 1986;488:19–32. [PubMed: 3034115]
36. Sheehan TE, Kumar PA, Hood DA. Tissue-specific regulation of cytochrome c oxidase subunit expression by thyroid hormone. Am.J.Physiol Endocrinol.Metab 2004;286:E968–E974. [PubMed: 14970006]
37. Arnold S, Goglia F, Kadenbach B. 3,5-Diiodothyronine binds to subunit Va of cytochrome-c oxidase and abolishes the allosteric inhibition of respiration by ATP. Eur.J.Biochem 1998;252:325–330. [PubMed: 9523704]

38. Arnold S, Kadenbach B. The intramitochondrial ATP/ADP-ratio controls cytochrome c oxidase activity allosterically. FEBS Lett 1999;443:105–108. [PubMed: 9989584]
39. Kadenbach B, Arnold S. A second mechanism of respiratory control. FEBS Lett 1999;447:131–134. [PubMed: 10214932]
40. Ludwig B, Bender E, Arnold S, Huttemann M, Lee I, Kadenbach B. Cytochrome C oxidase and the regulation of oxidative phosphorylation. Chembiochem 2001;2:392–403. [PubMed: 11828469]
41. Krieg RC, Knuechel R, Schiffmann E, Liotta LA, Petricoin EF III, Herrmann PC. Mitochondrial proteome: cancer-altered metabolism associated with cytochrome c oxidase subunit level variation. Proteomics 2004;4:2789–2795. [PubMed: 15352252]
42. Biswas G, Guha M, Avadhani NG. Mitochondria-to-nucleus stress signaling in mammalian cells: nature of nuclear gene targets, transcription regulation, and induced resistance to apoptosis. Gene 2005;354:132–139. [PubMed: 15978749]
43. Jahangir Tafrechi RS, Svensson PJ, Janssen GM, Szuhai K, Maassen JA, Raap AK. Distinct nuclear gene expression profiles in cells with mtDNA depletion and homoplasmic A3243G mutation. Mutat.Res 2005;578:43–52. [PubMed: 16202796]
44. Marusich MF, Robinson BH, Taanman JW, Kim SJ, Schillace R, Smith JL, Capaldi RA. Expression of mtDNA and nDNA encoded respiratory chain proteins in chemically and genetically-derived Rho0 human fibroblasts: a comparison of subunit proteins in normal fibroblasts treated with ethidium bromide and fibroblasts from a patient with mtDNA depletion syndrome. Biochim.Biophys.Acta 1997;1362:145–159. [PubMed: 9540845]
45. Diaz F, Fukui H, Garcia S, Moraes CT. Cytochrome c oxidase is required for the assembly/stability of respiratory complex I in mouse fibroblasts. Mol.Cell Biol 2006;26:4872–4881. [PubMed: 16782876]
46. Vonck J, Schafer E. Supramolecular organization of protein complexes in the mitochondrial inner membrane. Biochim.Biophys.Acta 2009;1793:117–124. [PubMed: 18573282]
47. Schafer E, Seelert H, Reifschneider NH, Krause F, Dencher NA, Vonck J. Architecture of active mammalian respiratory chain supercomplexes. J.Biol.Chem 2006;281:15370–15375. [PubMed: 16551638]
48. cin-Perez R, Fernandez-Silva P, Peleato ML, Perez-Martos A, Enriquez JA. Respiratory active mitochondrial supercomplexes. Mol.Cell 2008;32:529–539. [PubMed: 19026783]
49. Genova ML, Pich MM, Biondi A, Bernacchia A, Falasca A, Bovina C, Formiggini G, Parenti Castelli G, Lenaz G. Mitochondrial production of oxygen radical species and the role of Coenzyme Q as an antioxidant. Experimental Biology And Medicine (Maywood, N.J.) 2003;228:506–513.
50. Liu Y, Fiskum G, Schubert D. Generation of reactive oxygen species by the mitochondrial electron transport chain. Journal Of Neurochemistry 2002;80:780–787. [PubMed: 11948241]
51. Turrens JF. Superoxide production by the mitochondrial respiratory chain. Biosci.Rep 1997;17:3–8. [PubMed: 9171915]
52. Andreyev AY, Kushnareva YE, Starkov AA. Mitochondrial metabolism of reactive oxygen species. Biochemistry (Mosc.) 2005;70:200–214. [PubMed: 15807660]
53. Khalimonchuk O, Bird A, Winge DR. Evidence for a pro-oxidant intermediate in the assembly of cytochrome oxidase. J.Biol.Chem 2007;282:17442–17449. [PubMed: 17430883]
54. Li Y, Park JS, Deng JH, Bai Y. Cytochrome c oxidase subunit IV is essential for assembly and respiratory function of the enzyme complex. J.Bioenerg.Biomembr 2006;38:283–291. [PubMed: 17091399]
55. Radford NB, Wan B, Richman A, Szczepaniak LS, Li JL, Li K, Pfeiffer K, Schagger H, Garry DJ, Moreadith RW. Cardiac dysfunction in mice lacking cytochrome-c oxidase subunit VIaH. Am.J.Physiol Heart Circ.Physiol 2002;282:H726–H733. [PubMed: 11788423]

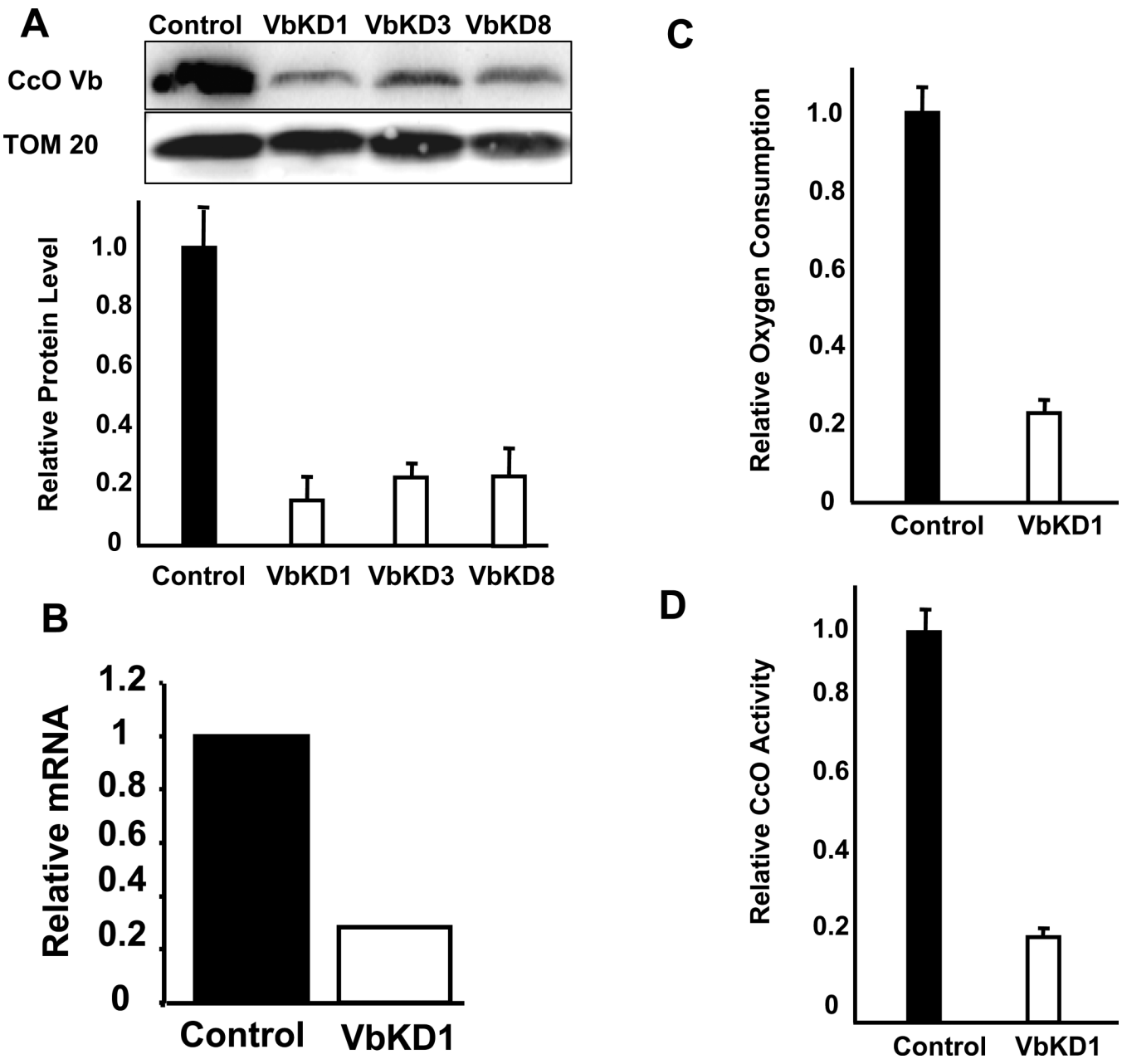

Figure 1. siRNA mediated silencing of *CcO Vb mRNA in RAW 264.7 macrophages*

A. 50 μg of mitochondrial protein from clones 1, 3 or 8 stably expressing siRNA against CcO Vb mRNA, or the scrambled siRNA (control), were subjected to immunoblot analysis using monoclonal antibodies to CcO Vb or TOM 20 proteins. The protein level was quantitated using Bio-Rad Versa Doc imaging software by normalizing the intensity of the CcO Vb band to that of TOM 20. ***B***. The level of CcO Vb mRNA from clone exhibiting the lowest protein level (VbKD1) was assayed using Real Time-PCR. The CcO Vb level was normalized to the β-actin mRNA level and is represented as the amount relative to that of control. ***C, D***. CcO activity in Vb KD1 cells was determined by measuring the rate of oxygen consumption (***C***) and the rate of cytochrome c oxidation (***D***). The relative activities were calculated based on 2.1 μmole cytochrome C oxidized/min/mg protein in C and 118 μmole of O_2 consumed/min/μg protein

in D, considered to be 1. For both assays, the slope of the linear portion of triplicate experiments was averaged and the value of the control experiments was arbitrarily set to one.

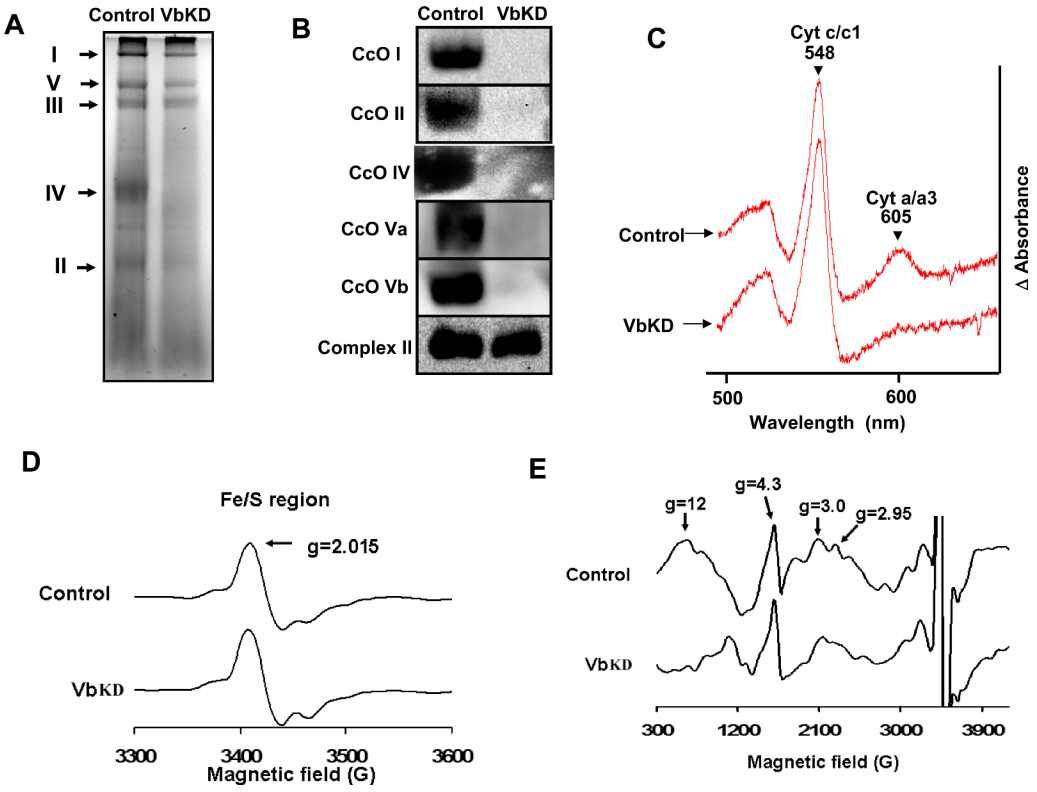

Figure 2. Silencing of subunit Vb leads to loss of CcO

A, 100 μg of mitochondrial extract was separated using 6-13% BN-PAGE and stained bands were visualized, **B**, 150 μg of mitochondrial protein was resolved on BN-PAGE as in A and transferred to PVDF membrane and probed with monoclonal antibodies for CcO I, CcO II, CcO IV, CcO Va, CcO Vb proteins. Complex II was used as loading control. ***C.*** 800 μg of mitochondrial protein solubilized with 2% lauryl maltoside was used for spectral analysis. The reduced-minus oxidized difference spectra was recorded and analyzed for the a/a3 specific peak at 605 nm and the cytochrome c/c1 peak at 548 nm. **D.** X-band EPR of the normal and VbKD cells were measured at 10 K using 5 mW microwave power as described in Materials and Methods. **D** show the Fe/S cluster and **E** shows the heme a, and heme a3/CuB binuclear center of CcO respectively.

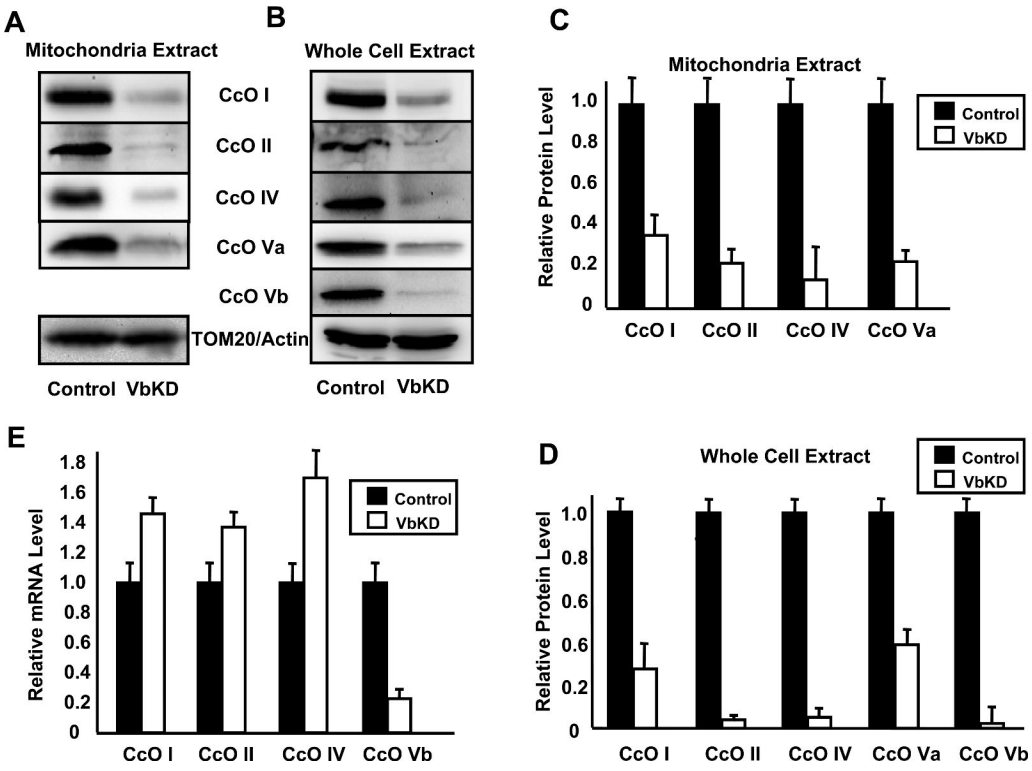

Figure 3. CcO Vb silencing caused a reduction in the steady state levels of other CcO subunits

A,B. 50 μg (mitochondrial extract) or 80 μg (whole cell extract) protein from control and VbKD1 cells were subjected to immunoblot analysis using monoclonal antibodies for CcO subunits I, II, IV, Va, and Vb, and either TOM 20 for mitochondrial samples or β-actin for whole cell extract as loading controls. ***C,D.*** The protein levels for various subunits were quantitated as described in Figure 1A. ***E.*** The mRNA levels for indicated CcO subunits were determined using Real Time-PCR. The mRNA levels were normalized to β-actin and the level of each subunit present in control was arbitrarily set at one.

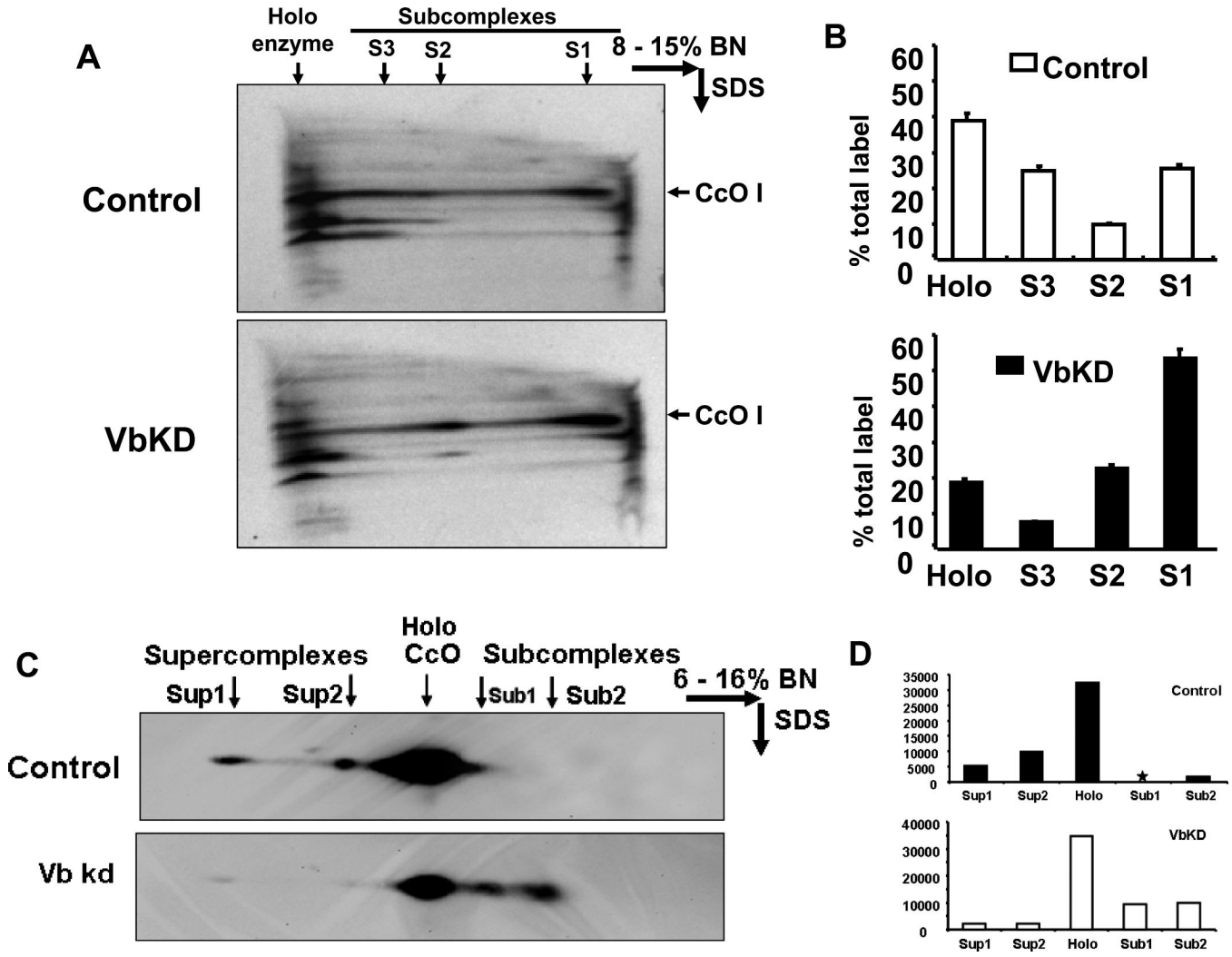

Figure 4. Accumulation of subcomplexes of CcO in VbKD cells

A. Two dimensional BN PAGE/SDS analysis of mitochondrial samples from metabolically labeled cells. Cells were labeled with 20 μCi S^{35}-Methionine in presence of 30 μg/ml cycloheximide for 2h and chased for 3h with excess unlabeled Met. CcO subcomplexes (S1, S2 and S3) are indicated. Autoradiogram of SDS gel has been presented. **B.** Quantitation of the bands from A. The sum of the band intensities of the holoenzyme and subcomplexes was taken as 100% for calculating the % distribution. **C.** Two dimensional BN PAGE/SDS analysis of subcomplexes and supercomplexes. 150 μg of mitochondrial protein was used in each case and CcO I antibody was used for probing the blot. An SDS gel pattern is presented. **D**. Quantitation of the bands from **C**.

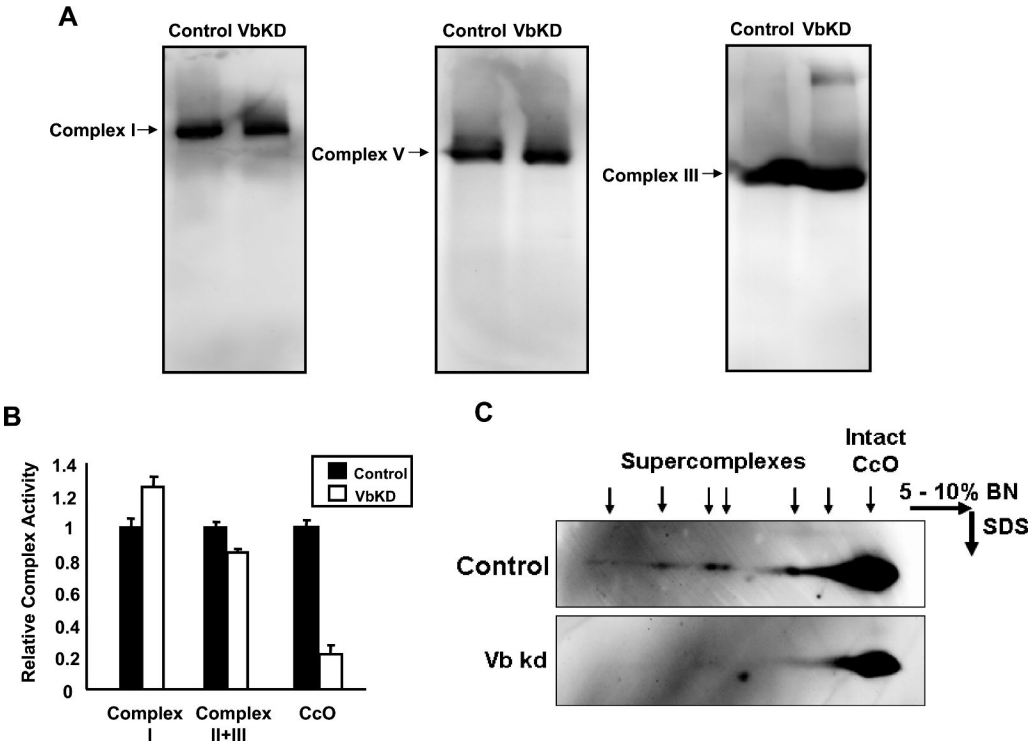

Figure 5. Levels of other electron transfer chain complexes and loss of supercomplexes in VbKD cells

A. Resolution of complexes I, III and V from control and VbKD cells by blue native gel analysis. Details were as in Figure 2 and the Materials and Methods section. **B.** Relative activities of complexes I, II + III and CcO in control and Vb KD cells. 50 μg protein was used in each case as described in the Materials and Methods section. The relative activities were calculated based on 2.1 μmole cytochrome C oxidized/min/mg protein for CcO, 265 nmoles NADH oxidized/min/mg protein for complex I and 218 nmoles cytochrome C reduced/min/mg protein for complex II/III, considered as 1. **C.** Immunoblots showing supercomplexes in control and VbKD mitochondria separated by two dimensional Blue Native gel analysis. The blots were probed with CcO subunit I antibody.

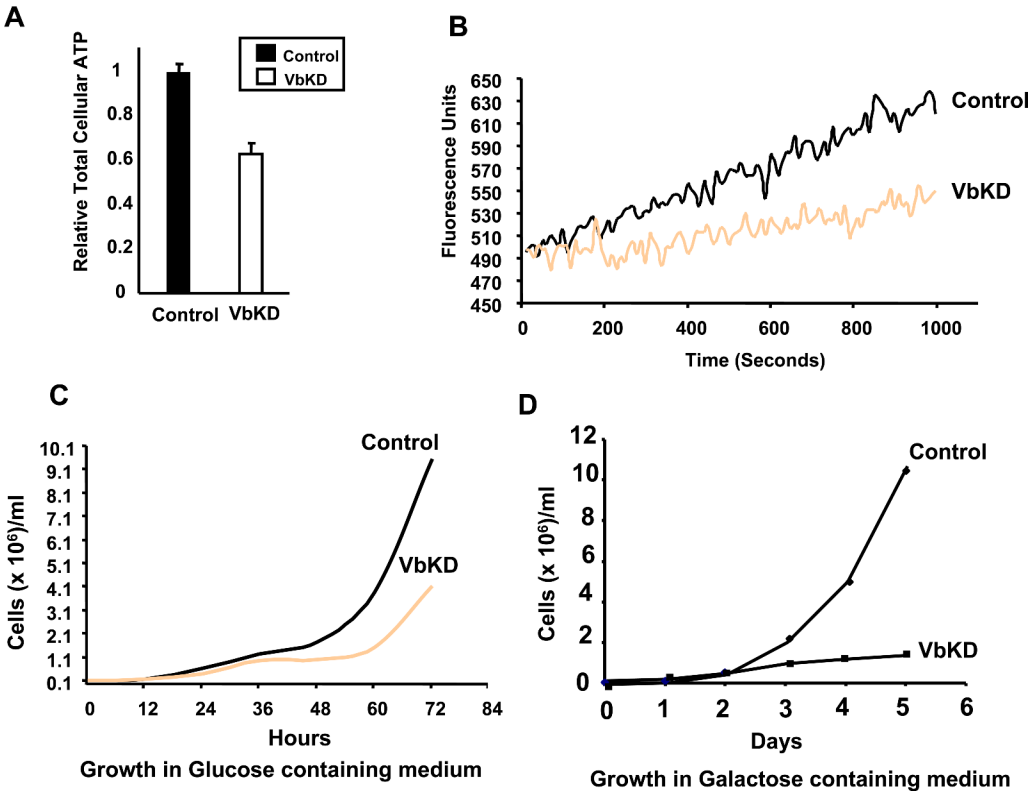

Figure 6. Impaired mitochondrial function and growth defects in VbKD cells

A. Relative cellular ATP levels in control and VbKD cells. ATP was measured in 10^6 cells using Somatic cell assay kit, as described in Materials and Methods. The relative ATP level was calculated based on 2.9 nmoles of ATP/ 10^6 cells considered as 1. **B**. Spectrofluorometric analysis of mitochondrial membrane potential ($\Delta\Psi m$) following the uptake of mitotracker orange (50 nM), as described in Materials and Methods. Excitation at 525 nm and emission at 575 nm were followed. **C, D.** Growth rates of control and VbKD cells in normal medium (C) and galactose medium (D).

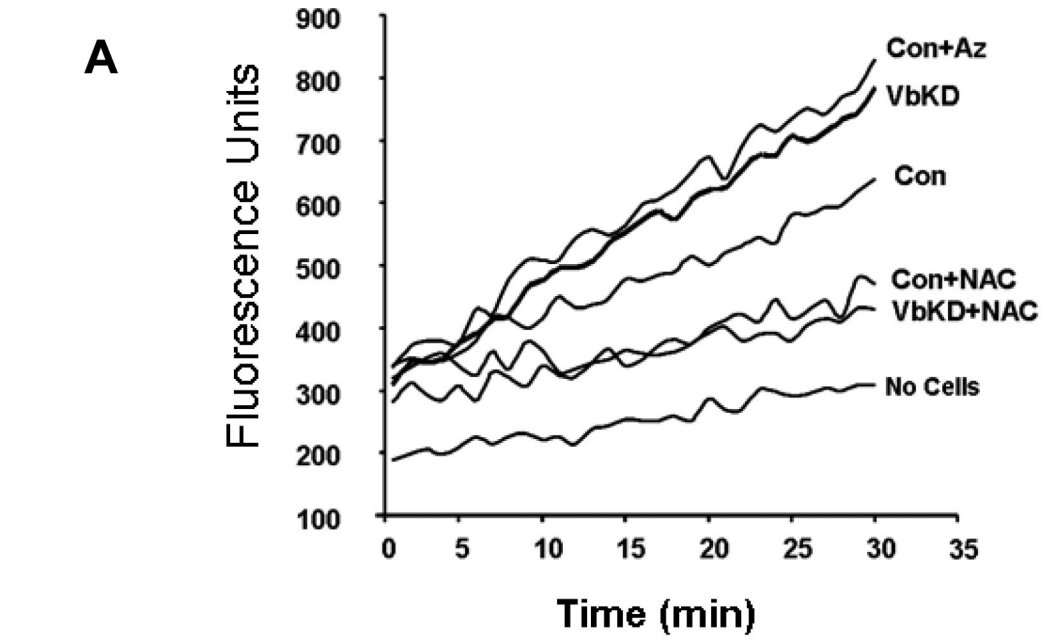

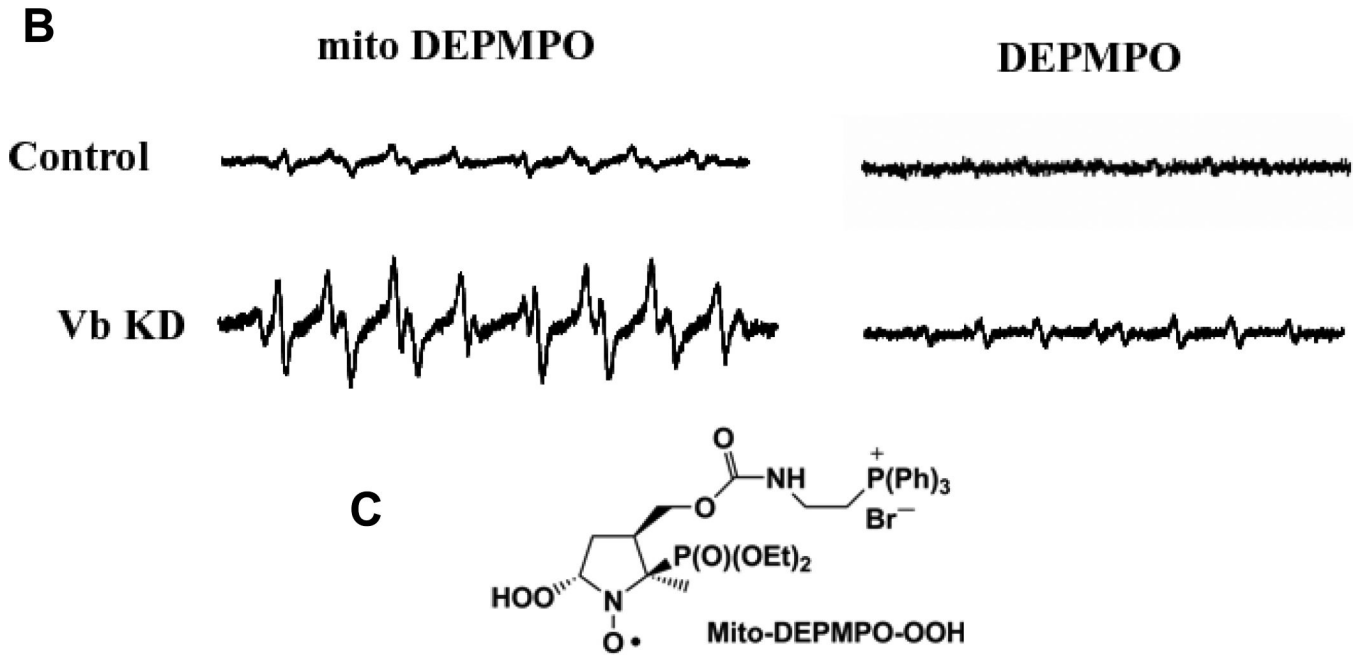

Figure 7. Increased mitochondrial ROS formation in VbKD cells

A. Formation of ROS in isolated mitochondria from control and VbKD cells measured by DCFDA oxidation. Azide (Az, 1mM), N-Acetyl Cysteine (NAC, 10mM) were added at 0 time. **B**. EPR spectrum obtained from isolated mitochondria following spin trapping with mito-DEPMPO or DEPMPO. Mitochondria (200 μg) were incubated with Mito-DEPMPO (50 mM) in phosphate buffer at pH 7.3 for 20 min at 37 °C. **C**. Structure of the adduct of superoxide and mito-DEPMPO